Tissue and Cell 87 (2024) 102330

Contents lists available at ScienceDirect

Tissue and Cell

journal homepage: www.elsevier.com/locate/tice

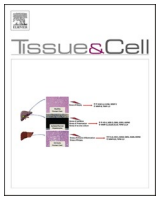

Modulation of the Sirtuin-1 signaling pathway in doxorubicin-induced nephrotoxicity (synergistic amelioration by resveratrol and pirfenidone)

Samia Mahmoud Manawy [a], Eman Mohamed Faruk [b,c,*], Rabab Fawzy Hindawy [d], Mahmoud M. Hassan [e], Diaa M.G. Farrag [f], Mansour A.E. Bashar [f], Hanan Fouad [g,h], Rania Abubaker Bagabir [i], Dina Allam Abdelmaksoud Hassan [j], Ahmed Mohammed Zaazaa [k], Mohamed Ghazy Attia Hablas [l], K Mostafa Kamal [a]

[a] Department of Anatomy and Embryology, Faculty of Medicine, Benha University, Benha, Egypt
[b] Anatomy Department, College of Medicine, Umm Al-Qura University, Makkah, Saudi Arabia
[c] Department of Histology and Cell Biology, Faculty of Medicine, Benha University, Benha, Egypt
[d] Department of Forensic Medicine and Clinical Toxicology, Faculty of Medicine, Benha University, Benha, Egypt
[e] Department of Physiology, Faculty of Medicine, Benha University, Benha, Egypt
[f] Marine Biology Branch, Zoology Department, Faculty of Science, Al-Azhar University, Nasr City, Cairo 11884, Egypt
[g] Basic Medical Sciences, Faculty of Medicine, Galala University, Galala City, POB 43711, ATTAKA, Suez Governorate, Egypt
[h] Department of Medical Biochemistry, Faculty of Medicine, Cairo University, Cairo POB 12613, Egypt
[i] College of Medicine, Hematology and Immunology Department, Umm Al-Qura University, Makkah, Saudi Arabia
[j] Histology and Cell Biology Department, Faculty of Medicine for Girls, Al-Azhar University, Egypt
[k] Students at Faculty of Medicine, Benha National University, Benha Colleges in Cairo, Egypt
[l] Department of Histology and Cell Biology, Faculty of Medicine, Suez University, Suez, Egypt

A R T I C L E I N F O

Keywords:
Doxorubicin
Renal toxicity
Sirtuin-1
Resveratrol
Pirfenidone

A B S T R A C T

The current study was conducted to determine the precise mechanisms of Sirtuin-1 (Sirt-1), TGF- β (Transforming Growth Factor-β), and long non-coding RNA Metastasis Associated Lung Adenocarcinoma Transcript 1 (LncRNA MALAT-1) in signaling pathways in doxorubicin (DOX)-induced nephrotoxicity. The potential therapeutic effect of Resveratrol and Pirfenidone in DOX toxicity was also assessed. Thirty-six male adult rats were evenly distributed into four groups: Group 1: control rats. Group 2: DOX exposed rats' group, each animal received 7.5 mg/kg DOX as a single intravenous dose, Group 3: DOX exposed group subjected to oral resveratrol (20 mg/kg/daily for two weeks), Group 4: DOX exposed group subjected to oral Pirfenidone (200 mg/kg once daily for 10 days). At the planned time, animals were sacrificed. Renal tissue was collected to assess matrix metalloproteinase-9 (MMP9), inflammatory and apoptotic markers: tumor necrosis factor-alpha (TNF- β, caspase-3, cyclo-oxygenase-2 (COX-2), and oxidative stress markers: nitric oxide (NO), Glutathione (GSH), malondialdehyde (MDA), and superoxide dismutase (SOD). Sirtuin-1 (Sirt-1), TGF-β, and LncRNA MALAT-1 were quantitatively assessed by real-time RT-PCR in the whole blood. Results showed that the DOX group exhibited a significant increase in oxidative stress markers, and inflammatory, and apoptotic markers in the renal tissue. Histologically, the renal tubule lining cells exhibited vacuolar alterations in the cytoplasm, glomerular atrophy, and vascular congestion. Furthermore, renal degeneration was evident, as confirmed by the heightened immunoexpression of MMP9. Exposure to DOX resulted in a significant decrease in Sirtuin-1 (Sirt-1) with a significant increase in the TGFβ, and LncRNA MALAT-1 gene expression. However, pre-treatment with either resveratrol/or Pirefenidone ameliorated the histological renal alterations, regulated the pathways of Sirt-1, TGFβ, and LncRNA MALAT-1, and decreased all oxidative stress, inflammatory and apoptotic markers. In conclusion, DOX exposure leads to renal toxicity by inducing renal degeneration, oxidative stress, and apoptosis. Administration of either resveratrol or Pirfenidone counteracted these changes and protected the kidney against DOX-induced renal damage.

* Corresponding author at: Anatomy Department, College of Medicine, Umm Al-Qura University, Makkah, Saudi Arabia.
E-mail addresses: samia.manawy@fmed.bu.edu.eg (S.M. Manawy), emkandel@uqu.edu.sa (E.M. Faruk), dr-rababhidawi@yahoo.com (R.F. Hindawy), diaa.magdy@azhar.edu.eg (D.M.G. Farrag), dr_mb2020682@azhar.edu.eg (M.A.E. Bashar), hanan.fouad@kasralainy.edu.eg (H. Fouad).

https://doi.org/10.1016/j.tice.2024.102330
Received 8 January 2024; Received in revised form 8 February 2024; Accepted 13 February 2024
Available online 20 February 2024

1. Introduction

Doxorubicin (DOX, also known as Adriamycin) is a potent antitumor antibiotic used to treat various malignant tumors. DOX has many hazards and side effects involving several organs (Shao et al., 2019). One of these dangerous side effects is its adverse effect on the kidney (Ikewuchi et al., 2021). It is one of the drugs that cause acute kidney injury, and nephrotoxicity that leads to a life-threatening impact (Afsar et al., 2020).

DOX (Adriamycin) mediates nephrotoxicity via induction of oxidative stress, inflammatory changes, and induction of apoptosis (El-Sayed et al., 2017; Songbo et al., 2019). Its oxidative stress action has a deleterious impact affecting several organs such as the liver, heart, and kidney (Songbo et al., 2019). Accumulation of DOX inside renal tubules contributes to its direct degenerative mechanism in the kidney (Yalcın et al., 2023).

Resveratrol (RVS) is a phytoalexin present in a minimum of 72 plant species, several of which humans consume, such as mulberries, grapes, and peanuts. Resveratrol acts as an antioxidant and it is part of a group of members known as polyphenols (Singh et al., 2019). Resveratrol has several health benefits as it can act as an anti-inflammatory, cardioprotective, and antioxidant. Studies have proven its potential therapeutic effects on heart and kidney diseases (Singh et al., 2019; Den Hartogh and Tsiani, 2019; Shahbazi et al., 2020).

Pirfenidone, which is orally effective, is a modified phenyl pyridine with the ability to traverse cell membranes independently of receptor assistance. It is easily taken up from the gastrointestinal tract following oral intake. A recent study proved that pirfenidone suppresses DOX-induced renal damage through inhibition of MCP-1 and JNK1 signaling pathways. Although it is unclear in detail how pirfenidone modulates fibrogenesis, its effects are likely to possess multiple targets, pirfenidone exhibits antioxidant properties as well as anti-transforming growth factor (anti-TGF) and anti-platelet-derived growth factor effects. It appears to be generally safe for use in chronic fibrotic disorders, multiple sclerosis, chronic hepatitis C, and chronic allograft rejection (Lopez et al., 2015; Hazem et al., 2022a).

Pirfenidone does not have a direct antihypertensive effect, but it was reported to decrease the expression of mineralocorticoid receptors and prevent angiotensin II-induced cardiac hypertrophy in hypertensive mice (Hazem et al., 2022a). As regards resveratrol, the antihypertensive or vasorelaxant effects of resveratrol have been attributed to increased expression of endothelial nitric synthase, improved nitric oxide (NO) release, and endothelium-dependent vasorelaxation, 2 decreased endothelin-1 and angiotensin II production,7 decreased sympathetic activity,8 and decreased oxidative stress (Mozafari et al., 2015).

Sirtuins exist in seven variations, designated as SIRT1–SIRT7, each distinguished by their specific locations. SIRT1, the most well-known variant, exerts its influence on proteins through NAD+ coenzymes, associating it with cellular energy metabolism and the 'redox' state. Deficiencies in SIRT1 are implicated in various medical conditions, including diabetes mellitus, cardiovascular diseases, neurodegenerative syndromes, and kidney diseases, especially during stressful situations (Dou and Zhao, 2022). In kidney disorders, SIRT1 promotes cell survival in affected kidneys by modulating responses to diverse stress stimuli. It also participates in arterial blood pressure control, guards against cellular apoptosis in renal tubules through catalase induction, and initiates autophagy. Growing in vitro and in vivo evidence suggests that SIRT1 activity is directed, among other functions, towards nephroprotection. Consequently, SIRT1 is potentially a novel therapeutic element in addressing age-related renal diseases, including diabetic nephropathy (Stojanović et al., 2022).

The current study was conducted to evaluate the potential therapeutic effects of resveratrol and pirfenidone on DOX-induced nephrotoxicity through assessment of their effects on Sirtuin-1 (Sirt-1), TGF-β, LncRNA MALAT-1 signaling pathway, apoptotic and inflammatory markers.

2. Material and method

2.1. Experimental animals

Ethical approval No.12–6–2023 was obtained from Banha University Faculty of Medicine, Egypt, for all animal procedures. The study was conducted on 36 adult male Sprague Dawley rats, 6–8 weeks old (200–220 g). Animal experiments were conducted at the Experimental Animal Unit of the Faculty of Medicine at Banha University. During the experiment, animals were kept at a suitable temperature (21±2 °C) and humidity (60%), with 12 hours of dark light alternated with unrestricted access to food and water. The animals were fed balanced diets. We conducted all animal procedures under the Declaration of Helsinki (2008) and the guidelines of Cairo University's Ethical Committee for the care and use of laboratory animals. Before starting the experiments, the animals were acclimatized to laboratory conditions for 1 week.

2.2. Chemicals and drugs

The DOX was purchased from Sigma Chemical Company (St. Louis, MO, USA) as DOX hydrochloride (2 mg/ml). Resveratrol (99% purity) was delivered from Sigma Chemicals Company (St. Louis, MO, USA) (CAS Number: 501–36–0). Pirfenidone (200 mg tab) was delivered from Sigma Chemical Company (St. Louis, Mo.) with CAS number 53179–13–8. Most chemicals and reagents were sourced from Sigma Chemical Company (St. Louis, MO, USA).

2.3. Preparation and dosage of resveratrol, and pirfenidone

Resveratrol was prepared in a normal saline solution and given to rats at a dose of (20 mg/kg body weight/day) for 14 successive days (Yalcın et al., 2024).

pirfenidone (PFD) tablets were ground and suspended in 1% carboxymethyl cellulose. One pirfenidone tablet was dissolved in 4 ml CMC to obtain a final concentration of 50 mg/ml and was given in a dose of 200 mg/kg/d oral gavage for two weeks [16&17].

2.4. Experimental design and animal grouping

Thirty-six adult male rats (200–220 gm) were divided equally into four groups (nine rats per group): Group 1(G1) represents control and received saline. Group 2(G2) represents pathological control and received a single dose of DOX (7.5 mg/kg) in the tail vein (El-Sayed et al., 2017). Group 3(G3) included DOX-exposed rats and they were given resveratrol (20 mg/kg B wt/day) orally for two weeks (Yalcın et al., 2024). Group 4(G4) included the DOX-exposed group and received pirfenidone (200 mg/kg of body weight once daily for 10 days) orally by a gastric gavage (Hazem et al., 2022b; Morsi et al., 2023; Fouad et al., 2021). (Diagram 1.).

2.5. Assessment of blood pressure

The blood pressure was measured as previously reported (Chen et al., 2012). A 2 mg/kg intraperitoneal injection of ethyl carbamate was used to sedate the animals. Systolic blood pressure was evaluated using tail-cuff plethysmography on three occasions (Letica LE 5100, pain lab, Barcelona, Spain), and the average of these three measurements was documented.

2.6. Serum and tissue preparation

At the end of the experiment (two weeks after the DOX injection), blood samples were obtained from the retro-orbital venous plexus using nonheparinized tubes after anesthetizing the rats with light ether. The serum samples underwent centrifugation at 4000x g for 20 minutes and were subsequently stored at –20 °C. After that, all animals were

sacrificed in all groups and the right kidney was collected in PBS (0.5 M, pH 7.4) for enzyme and gene expression studies, while the left kidney was preserved in 10% formalin saline for histopathological analysis. The kidneys were rapidly removed, rinsed with ice-cold saline, and then stored at –80°C until homogenization in ice-cold KCl using a sonicator homogenizer. The centrifuged homogenate was divided into aliquots for the measurement of caspase-3, kidney tumor necrosis factor-alpha (TNF-α), cyclo-oxygenase-2 (COX-2), Glutathione (GSH), malondialdehyde (MDA), and the enzyme activity of superoxide dismutase (SOD).

2.7. Biochemical analysis

Aqueous primary standards were used to measure serum urea and creatinine spectrophotometrically (Bio-diagnostic, Egypt). The total NO production is the sum of its metabolite's nitrite and nitrate (Nade et al., 2013). Serum NO concentration was measured by the enzymatic assay in serum using the reagent kit (Nitric oxide colorimetric assay, 1-756-281, Roche Diagnostics, Mannheim, Germany). TNF-α, SOD, and caspase-3 activity in renal tissue were measured using commercial assay kits (TNF-α-CAS 94948-59-1, 19160-1KT-F, and CASP3C, NA.84. Sigma-Aldrich Co., St Louis, MO, USA) and COX-2 ELISA kit (Cat. No. E-EL-H5574, Elabscience Biotechnology, USA). Renal tissue MDA was analyzed using a commercial assay kit (MAK085, Sigma-Aldrich, USA). Moreover, GSH was assayed in renal tissue using a commercial kit from Biodiagnostics (Cat No. GR 25 11).

2.8. Assay of gene expression levels of Sirtuin-1 (Sirt-1), TGF-β and LncRNA MALAT-1 genes

2.8.1. Real-time PCR

The RT-PCR Master Mix kits were used (ThermoFisher, Cat No. 4368814, Cat No. 4368708). To assess the reaction, we used a Step One System (RQ Manager 1.2, software v 2.1, Applied Biosystem). The amplification plot, Glyceraldehyde 3-phosphate dehydrogenase (GAPDH) was utilized to determine the threshold cycle (CT) value as the normalization control is the endogenous reference gene used to eliminate any contaminations. The thermal cycling profiles were 15 minutes at 45ºC for the synthesis of cDNA followed by 5 minutes at 95ºC for polymerase activation and reverse transcriptase inactivation. The arrangement of the primers for each gene present in the work was seen in Table 1 as the RNA sequences were obtained from GenBank, and the primer pairs were chosen using the sequences available on the website http://www.ncbi.nlm.nih.gov/tools/primer-blast. The criteria for selecting the optimal primer pair included factors such as a melting temperature (Tm) within the range of 60–65°C and an expected amplicon length of approximately 90–200 base pairs.

Table 1
Genes primers.

Gene symbol	Primer sequence	Gene bank accession number
Sirt-1	F: GGGATCTCTAGGCCCAGTTC R: CTTTGGGGAGAGGGGGAC	NM_001107073.1
TGF-β	F: TGCGCCTGCAGAGATTCAAG R: GGTAACGCCAGGAATTGTTGCTA	NM_021578.2
MALAT-1LncRNA	F: ACAGGACTCCATGGCAAACG R: AACGGATTTGGTCGTATTGGG	FO181540.13
GAPDH	F: AATGGTGAAGGTCGGTGTGAAC R: AGGTCAATGAAGGGGTCGTTG	NM_017008.4

2.8.2. Determination of relative quantification (relative expression)

The relative expression levels of all examined genes were determined through the comparative cycle threshold (Ct) method. The PCR data presents Ct values for both the target genes and the housekeeping gene (GAPDH). A negative control sample involved the absence of template cDNA. Data analysis was performed using the Applied Biosystems StepOneplus software. All values were normalized to the GAPDH housekeeping gene, and the results were expressed as fold changes relative to the baseline levels observed in the control samples (Wennmalm et al., 1993; Caraguel et al., 2011).

2.9. Light microscopic procedure

Each group's kidney specimen was embedded in paraffin and fixed in 10% neutral buffered formalin, followed by sections of 4–5 mm thickness. The sections underwent staining using hematoxylin and eosin (H&E), PAS staining, and matrix metalloproteinase (MMP)−9 immunostaining (Pinkaew et al., 2022; Kiernan, 2015; Liu et al., 2019).

To prepare slides for immunohistochemistry of MMP-9, Slices of renal paraffin (6um) were deparaffinized with xylene and rehydrated in graded ethanol solutions. Citrate buffer (pH 6.0) was used for antigen retrieval on rehydrated sections, followed by a phosphate-buffered saline wash, MMP-9 primary antibodies (Santa Cruz Biotechnology Inc., Santa Cruz, CA) smearing, and overnight incubation at 41°C. Secondary antibodies were used at 1:200 dilutions (biotinylated antihorse IgG, Vector Laboratories Inc.). The sections were placed on glass slides after being soaked in tap water, dehydrated in ordered alcohol, cleared with xylene, and mounted with coverslips. In the negative control sections, the main antibody was not applied. The MMP-9 immunoreaction was positive if brown nuclei were present. Light microscope photos were taken with a digital camera (Leica Qwin 500, Leica, England) (Nade et al., 2013; Wennmalm et al., 1993; Caraguel et al., 2011).

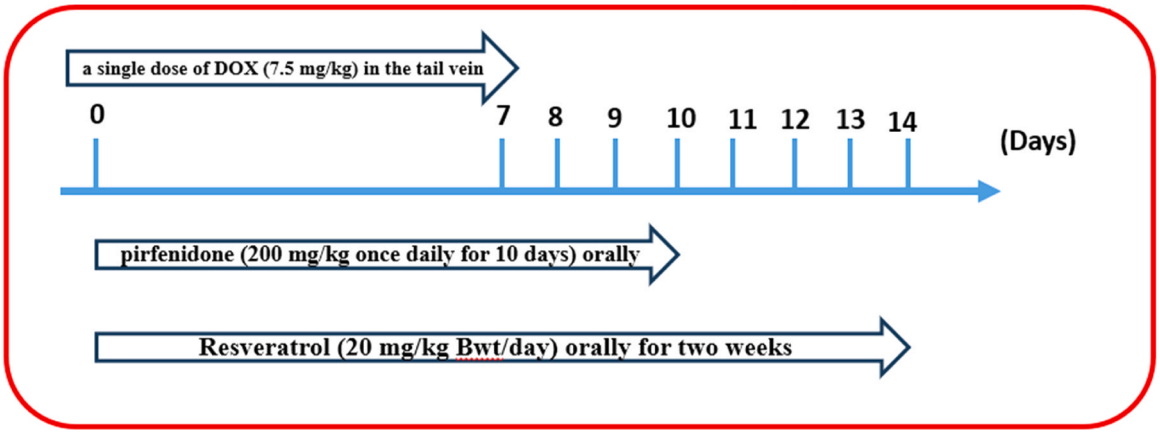

Diagram 1. Diagrammatic representation of the different time points of the current experiment.

2.10. Morphometric study

To determine the mean area percentages of PAS-stained structures and MMP-9 immunostaining, the Faculty of Medicine at Cairo University employed the Leica Qwin 500 image analysis computer system (Leica Microsystems Ltd, Cambridge, UK). Initially, the image analyser was calibrated automatically to convert pixels generated by the program into actual micrometer units. Ten non-overlapping fields were examined at a magnification of 400 per section., and three sections/animals were evaluated in each group. G*power software version 3.0.10 was employed to calculate sample size, with parameters set at a power of 80%, alpha level of 5%, and effect size of 0.55, based on prior studies and field expertise.

Image analysis involved automatic calibration to convert program-generated pixels to micrometer units (Faul et al., 2009).

2.11. Statistical analysis

The analysis of research data was conducted using GraphPad Prism (GraphPad Software, Version 8 for Windows, San Diego, California, USA). Shapiro's test for normality was employed to assess the normal distribution of values. The variables were presented as mean ± standard deviation. Group comparisons were performed using analysis of variance (ANOVA) and Tukey's post-hoc tests. Pearson correlations between various parameters in all rat groups were also carried out. Statistical significance was established for p-values less than 0.05.

3. Results

3.1. Mortality rate and body weight

The mortality rate was 11.11% in the DOX group as there was only one rat died in this group with no mortality in other groups during this study (control, DOX+ resveratrol, and DOX+ Pirfenidone groups).

3.2. Resveratrol and pirfenidone improved blood pressure and kidney function biomarkers following DOX administration in rats

A significant increase in systolic blood pressure (mmHg) and blood urea level (mg/dl), and a significant rise in serum creatinine level (mg/dl) were observed in the DOX group (G2) in comparison to the control group and the DOX+ resveratrol and DOX+ Pirfenidone groups (G3&G4) (P<0.001, each) (Table 2).

3.3. Resveratrol and pirfenidone improved renal status of oxidant/antioxidant biomarkers following DOX administration in rats

Administration of DOX significantly increased renal MDA levels and reduced renal GSH contents, and SOD activities as compared to the control group. Alternatively, treatment of DOX-exposed rats with either Resveratrol or Pirfenidone significantly ameliorated all markers of oxidative stress (Table 3).

Table 2
Impact of resveratrol or Pirfenidone treatment on systolic blood pressure, serum creatinine, and blood urea nitrogen (BUN) in the examined groups.

Groups/ parameter	Systolic blood pressure (mmHg)	Serum creatinine (mg/dl)	BUN (mg/dl)
Control group	118.1±0.01	0.79±0.02	23.15 ±0.23
DOX group	152±0.72[a]	1.91±0.01[a]	43.41 ±0.17[a]
Resveratrol +DOX group	139±0.17[bc]	1.01±0.01[bc]	30.91 ±0.01[bc]
Pirfenidone + DOX group	138±0.38[bc]	0.98±0.02[bc]	29.95 ±0.25[bc]

All data are presented as mean ± SD. [a] significant vs control group, [b] significant vs DOX group, [c] significant vs control group using one-way ANOVA followed by Tukey's post-hoc test, for multiple comparisons at P-value ≤ 0.05.

3.4. Resveratrol and pirfenidone improved renal inflammatory and apoptotic biomarkers following DOX administration in rats

There was a significant increase in NO, caspase-3, and COX-2 in DOX-treated rats, as well as a significant increase in TNF-α as compared to the control group. Compared to DOX-treated animals, the administration of Resveratrol or Pirfenidone facilitated the changes in COX-2, NO, caspase-3, and changes in TNF-α (Table 3).

3.5. Resveratrol and pirfenidone down-regulated renal LncRNA (MALAT-1) expression, and TGF-β expression and up-regulated renal Sirt-1 expression, following DOX administration in rats

There was a statistically significant decrease (p <.001) in gene expression of Sirt-1, and a significant increase in LncRNA (MALAT-1) gene, and TGF-β gene expression in the DOX-exposed group as compared to the control group. Resveratrol or Pirfenidone treatments significantly decreased the expression of the LncRNA (MALAT-1), and TGF-β and significantly increased Sirt-1 expression as compared to the DOX group. There was no significant difference in all genes' expression between control animals and those treated with either Resveratrol or Pirfenidone (Figs. 1 and 2).

3.6. Resveratrol and pirfenidone improved renal cortical histological changes following DOX administration in rats

Control rats displayed normal renal histoarchitecture with H&E stained. There was a normal capillary tuft surrounding the kidney corpuscles, as well as a patent Bowman's (filtration) space between them. Cuboidal cells with acidophilic granular cytoplasm, round vesicular nuclei, and intact apical brush borders were observed lining the proximal convoluted tubules (PCTs). The lumina of the distal convoluted tubules (DCTs) appeared wider (Fig. 3A).

In contrast, the group administered with DOX exhibited blood vessel congestion, focal haemorrhage between tubules, and degeneration of tubular epithelium with focal inflammatory cell infiltration in the cortical portion (Fig. 3B&C). While rats receiving Resveratrol or Pirfenidone supplementation reported fewer histological lesions after exposure to DOX. There was an almost complete restoration of the renal microstructure. Normal glomeruli and filtration spaces were seen in the

Table 3
Effect of resveratrol or Pirfenidone treatment on renal Inflammatory, apoptotic, and renal status of oxidant/antioxidant biomarkers in studied groups.

Groups/ parameter	Control group	DOX group	Resveratrol + DOX group	Pirfenidone + DOX group
MDA (nmol/g tissue)	8.51 ±0.01	34.32 ±0.72[a]	19.29±0.17[bc]	21.14±0.38[bc]
GSH (μmol/g tissue)	8.89 ±0.02	3.41 ±0.01[a]	6.71±0.01b[b]	7.01±0.02[b]
SOD (U/g tissue)	493.15 ±0.23	143.41 ±0.17[a]	441.91±0.01[b]	486.95±0.25[b]
NO (μmol/l)	1.51 ±0.01	4.12 ±0.72[a]	2.29±0.17[bc]	2.54±0.38[bc]
COX-2 (pg/ml)	38.89 ±0.02	102.91 ±0.01[a]	71.71±0.01[bc]	76.01±0.02[bc]
TNF-α (pg/ml)	23.15 ±0.23	83.41 ±0.17[a]	31.91±0.02[b]	29.95±0.25[b]
Caspase-3 (ng/ml)	0.74 ± 0.08	3.84 ± 0.05[a]	1.73± 0.01[bc]	1.87 ±0.03b[bc]

All values are expressed as mean ± SD, n = 9, [a] significant vs control group, [b] significant vs DOX group, [c] significant vs control group using one-way ANOVA followed by Tukey's post-hoc test, for multiple comparisons at P-value ≤ 0.05.

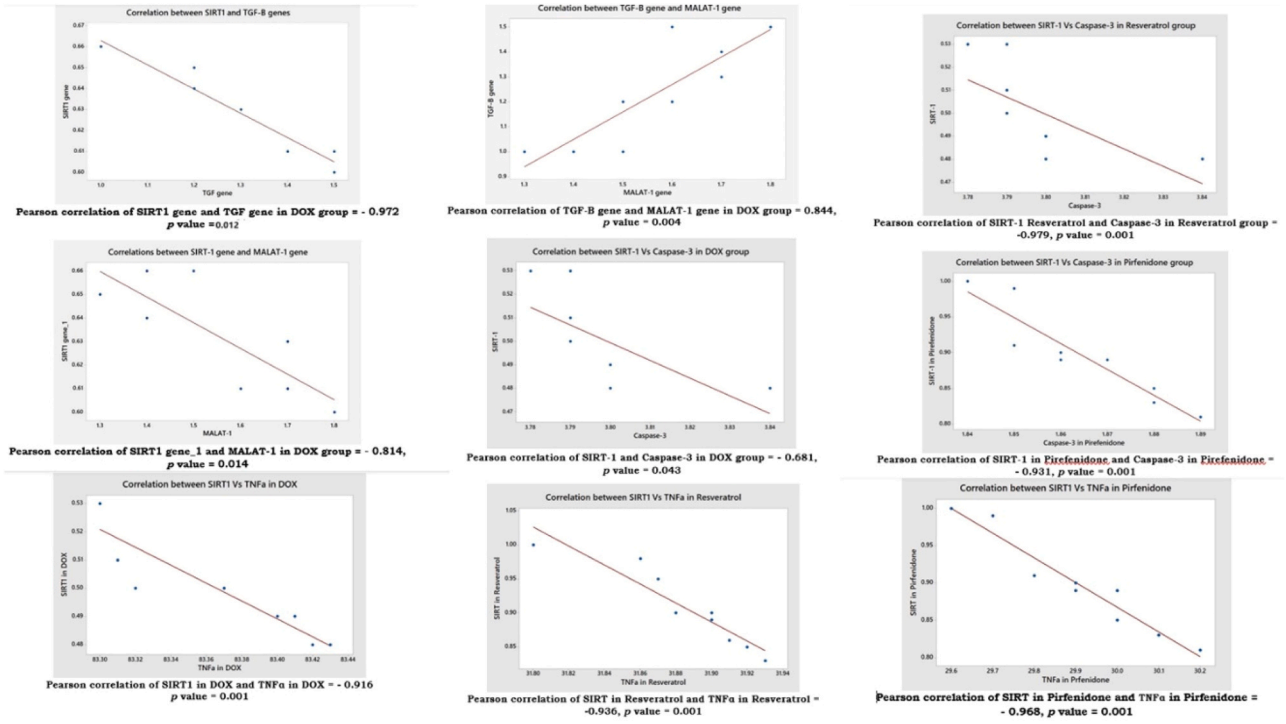

Fig. 1. Scatter blot between different studied parameters in all rat groups.

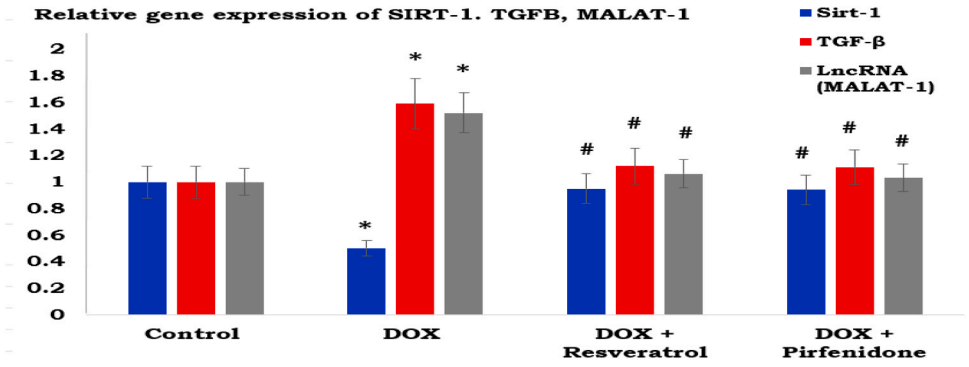

Fig. 2. Gene expression levels of SIRT-1, TGFβ, and MALAT-1 in the studied rat groups. * Indicates significance at $p < 0.05$ compared to the control group. # Indicates significance at $p < 0.05$ compared to the DOX group.

renal corpuscles. Tubules with intact brush borders were seen. There was only minor peritubular vascular congestion (Fig. 3D&E).

Regarding the PAS findings, a strong PAS reaction was observed in the glomeruli and renal tubules of the control group (Fig. 4A). On the other hand, the DOX-administered showed a reduced PAS-positive glomerular mesangial matrix and basal laminae as well as the tubular basement membranes (Fig. 4B). However, the DOX+ Resveratrol or DOX+ Pirfenidone groups showed increased glomerular and tubular PAS reactions (Fig. 4C&D).

3.7. Resveratrol and pirfenidone improved renal cortical degradation and remodeling of the extracellular matrix following DOX administration in rats

Regarding MMP-9 immunostaining, renal sections obtained from control animals exhibited a lack of immunoreaction (Fig. 5A). However, the DOX-administered group displayed a positive brown cytoplasmic MMP-9 immunoreaction in renal tissues (Fig. 5B). In contrast, sections from rats treated with both DOX+ resveratrol and DOX+ Pirfenidone showed a noticeable reduction in immunoreactivity in cortical renal tissues (Fig. 5C&D).

When DOX rats' sections were compared to control animals in renal tissue, the mean area percentages of brown MMP-9 immunostaining in cortical renal tissues significantly increased ($p<0.001$). Rats treated with both DOX+resveratrol and DOX+Pirfenidone had significantly reduced area percentages ($p<0.001$) (Fig. 5E).

3.8. Morphometric result

Concerning the mean area percentage of the PAS reaction, there was no notable difference between the control group and the rats treated with DOX+Resveratrol or DOX+Pirfenidone. However, a significant decrease ($p<0.001$) in the area percentage was observed in animals exposed to DOX compared to the control group. The groups treated with DOX+Resveratrol and DOX+Pirfenidone demonstrated a significant increase ($p<0.001$) in the mean area percentage of the PAS reaction compared to the DOX-exposed rats (Fig. 4E).

Regarding the mean area percentage of MMP-9 immunostaining, a

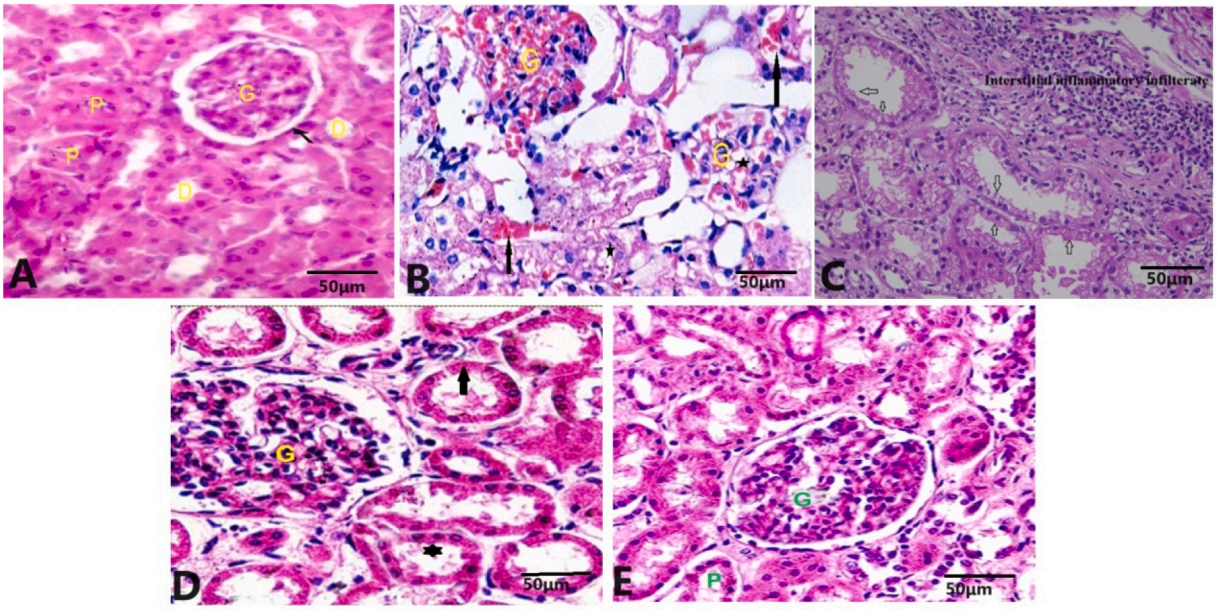

Fig. 3. (A) presents a micrograph of a renal cortex section from the control group, illustrating renal corpuscles with glomerular capillaries (G), the parietal layer of Bowman's space (arrow), and filtration spaces. Proximal convoluted tubules (P) exhibit a narrow lumen, acidophilic cytoplasm, and basal rounded nuclei. Distal convoluted tubules (D) display a wide lumen, less acidophilic cytoplasm, and rounded nuclei. In contrast, (B & C) depict micrographs of renal cortex sections from the DOX group, where the tubules are widely separated with an altered morphology. Some tubules exhibit multiple vacuoles (*), and nuclei are darkly stained, while others display karyolitic nuclei. The glomeruli appear expanded (G). Note the congested blood vessels (black arrows) and degenerated tubal epithelium (white arrows) with interstitial inflammatory cell infiltration. **(D)** A photomicrograph of a section of the renal cortex from the ***Resveratrol*** + ***DOX group*** showing normal tubules with acidophilic granular cytoplasm and rounded vesicular nuclei (arrow) with normal glomeruli (G). Some tubules show degenerative changes (star). **(E)** A photomicrograph of a section of the renal cortex from group ***Pirfenidone*** + ***DOX group*** showing a normal histological architecture for the renal tubules, and proximal convoluted tubules (p). Renal corpuscle showing minute degenerative changes with mild glomerulus hypercellularity (G). H&E, ×400.

significant increase ($p<0.001$) in the area percentage was observed in rats exposed to DOX compared to the control animals. However, treatment with Resveratrol or Pirfenidone significantly decreased ($p<0.001$) the mean area percentage of MMP-9 immunoexpression (Fig. 5E).

4. Discussion

Despite doxorubicin's benefits in reducing cancer mortality, it induces late-onset cardiomyopathy, hepatic damage, nephrotoxicity, and subsequent renal failure. Due to its widespread use in oncology, doxorubicin's toxic renal effects are considered significant clinical challenges (Shao et al., 2019; Ikewuchi et al., 2021).

Resveratrol, a nutraceutical, is a naturally occurring polyphenol present in red wine and grapes. Prior research has demonstrated its diverse beneficial biological properties, including anti-inflammatory, antioxidative, antiviral, and antitumor activities (Miguel Andressa et al., 2021; Beshay et al., 2020; Theodotou et al., 2017). The natural polyphenolic molecule RESV is an interesting candidate for the treatment of hypertension, as it mimics numerous molecular and biological effects of calorie restriction.

These facts coincided with our findings that resveratrol ameliorated the histological renal alterations elicited by doxorubicin, regulated the pathways of Sirt-1, TGFβ, and LncRNA MALAT-1, decreased all oxidative stress, inflammatory and apoptotic markers. Moreover, the antihypertensive or vasorelaxant effects of resveratrol have been attributed to increased expression of endothelial nitric synthase, improved nitric oxide (NO) release, and endothelium-dependent vasorelaxation, decreased endothelin-1 and angiotensin II production, decreased sympathetic activity, and decreased oxidative stress (Mozafari et al., 2015).

Pirfenidone (PFD) is a pyridone derivative known for its broad antifibrotic and anti-inflammatory effects. Through the modulation of various cytokines, PFD decreases the expression of intracellular adhesion molecule-1 (ICAM-1) and promotes the expression of anti-inflammatory cytokines such as IL-10 (Song et al., 2020). Previous research utilizing PFD in animal models of renal damage has shown promising outcomes, particularly in addressing tubulointerstitial fibrosis associated with conditions like unilateral ureteral obstruction (UUO) and diabetes (Armendariz-Borunda et al., 2012). These facts coincided with our findings that pirfenidone ameliorated doxorubicin-induced renal damage like the effects of resveratrol with no significant differences between both therapeutic interventions.

Although resveratrol exhibits protective effects against renal damage, it retains DOX cytotoxicity against tumor cells and increases tumor sensitivity to chemotherapy (RamachandraRao et al., 2009; Wu et al., 2022). DOX-induced nephropathy serves as a well-established and highly reproducible experimental model for proteinuric kidney diseases. Moreover, DOX has shown direct toxicity against tubular cells. Podocytes, integral components of the renal glomerular filtration barrier, are susceptible to injury and contribute significantly to the pathogenesis of proteinuria (Cotino-Nájera et al., 2023). These findings agree with our results that demonstrated doxorubicin elicited vacuolar changes in the cytoplasm of the renal tubule lining cells, glomerular atrophy, and vascular congestion. Moreover, renal degeneration was evident, as confirmed by the heightened immuno-expression of MMP9. Furthermore, there was a significant increase in blood pressure, creatinine, and BUN in the doxorubicin-exposed rat group.

Treatment with pirfenidone or Resveratrol improved blood pressure and kidney function biomarkers following DOX administration in rats. Due to pressure overload and left ventricular hypertrophy, doxorubicin treatment-induced cardiac hypertrophy and left ventricle dysfunction (Hekmat et al., 2021) and this explains the increase in systolic blood pressure in our study.

Resveratrol has multiple effects, including several positive vascular adaptations, such as reducing oxidative damage and improved hyperemic vasodilation, which correlate with the activation of eNOS. RESV activates adenosine monophosphate-activated protein kinase (AMPK),

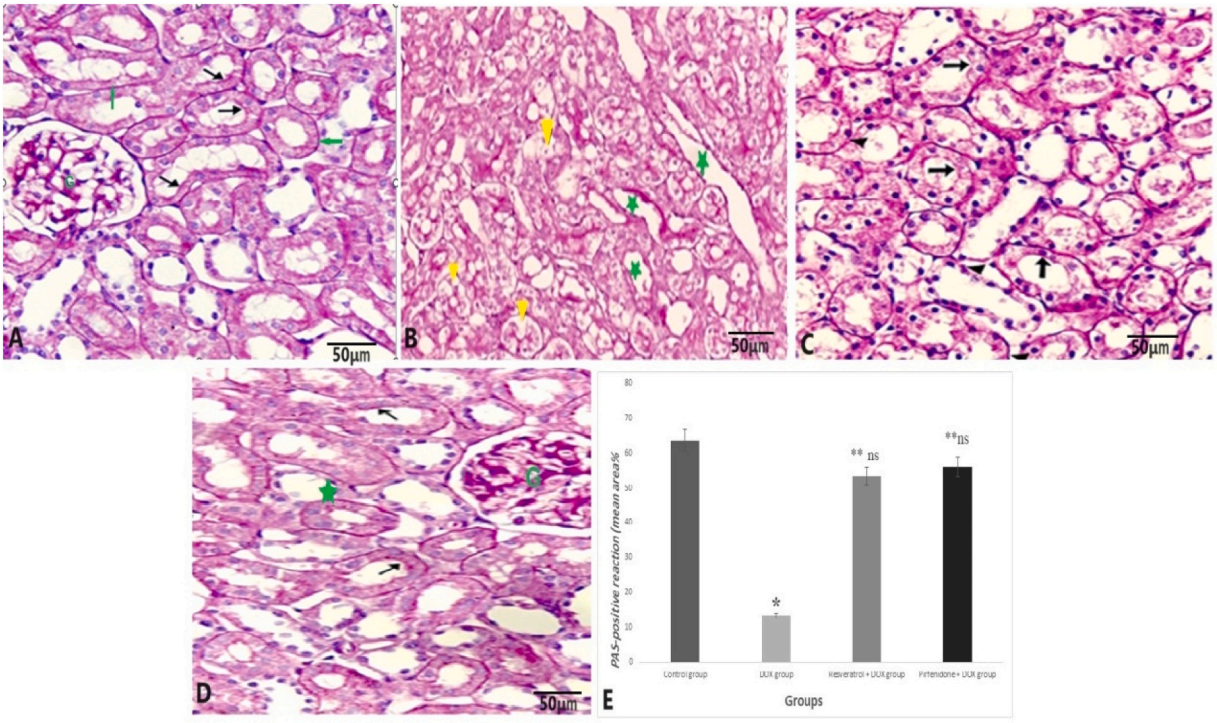

Fig. 4. (A) A micrograph of a renal cortex section from the control group depicts a positive Periodic acid–Schiff (PAS) reaction in the basement membranes of tubules (green arrow), in the brush border of the renal tubule (black arrow), and in the glomerular capillaries (G). (B) In contrast, a micrograph of a renal cortex section from the DOX group reveals a reduction in Periodic acid–Schiff (PAS) reactivity with a partial loss of the brush border in most tubules (green stars). The basement membrane is interrupted in almost all tubules, with positive PAS reactivity in the mesangial matrix (yellow stars). (C) Another micrograph from the Resveratrol + DOX group shows a positive Periodic acid–Schiff (PAS) reaction in many cortical tubules with a preserved brush border (arrows). A few tubules exhibit interrupted basement membranes (head arrows). (D) A micrograph from the Pirfenidone + DOX group displays many cortical tubules with preserved brush borders (arrow). Continuous basement membranes (star) are observed in nearly all tubules and the glomerular capillaries (G). PAS ×400. (E) Represents the mean area percentage of the PAS reaction. * Significant $p < 0.05$ in comparison to the control group. ** NS Nonsignificant $p > 0.05$ in comparison to the control group.

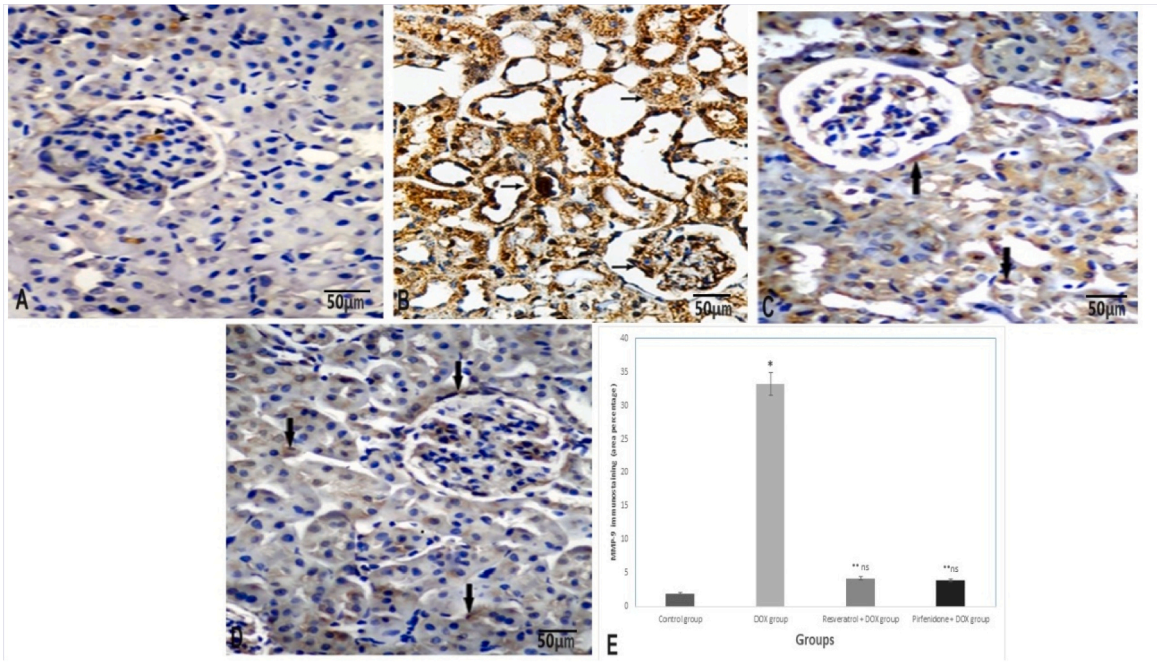

Fig. 5. (A) A micrograph of a renal cortex section from Group I (the control group) displays some positive MMP-9 immunoreactive nuclei within the tubular lining cells and glomerulus. (B) In contrast, a micrograph of a renal cortex section from the DOX group reveals significant MMP-9 immunopositivity in the cytoplasm and nuclei among the tubules and glomeruli (arrow). (C) Another micrograph from the Resveratrol + DOX group demonstrates an apparent decrease in MMP-9 immunoreactivity (arrows) in the tubular lining cells. (D) Similarly, a micrograph from the Pirfenidone + DOX group illustrates a reduction in MMP-9 immunoreactivity (arrows) in the tubular lining cells. (E) Represents the mean area percentage of the MMP-9 reaction. * Significant $p < 0.05$ in comparison to the control group. ** NS Nonsignificant $p > 0.05$ in comparison to the control group.

which directly phosphorylates eNOS, increasing NO production (Chen et al., 1999) Alternatively, NO can activate AMPK, placing eNOS upstream of AMPK (Zhang et al., 2008). In addition, RESV reduces oxidative damage to the heart, reduces cardiac left ventricular hypertrophy, and inhibits pro-hypertrophic signaling pathways (Dolinsky et al., 2010, 2013).

Pirfenidone does not have a direct antihypertensive effect, but it was reported to decrease the expression of mineralocorticoid receptors and prevent angiotensin II-induced cardiac hypertrophy in hypertensive mice (Yamazaki et al., 2012).

Moreover, another study stated that prophylactic administration of pirfenidone prevented acute kidney injury due to bilateral ischemia in rats. Recovery of NO production appears to be one of the mechanisms of the pirfenidone reno-protective effect (ima-Posada et al., 2019).

Pirfenidone is a small synthetic molecule with high oral bioavailability, exerting an antifibrotic activity, but also antioxidant and anti-inflammatory effects. These effects have been attributed to the inhibition of several growth factors (transforming growth factor-β, but also platelet-derived growth factor and beta fibroblast growth factor), matrix metalloproteinases, and pro-inflammatory mediators (such as interleukin-1β and tumor necrosis factor-α), and possibly also an improvement of mitochondrial function and modulation of lymphocyte activation (Mavrogiannis et al., 2022).

In the current study, DOX-exposed animals exhibited a significant decrease in GSH activity and SOD levels, accompanied by a significant increase in MDA, causing ROS to overproduce and oxidative damage to occur. Several studies suggest that DOX toxicity is caused by oxidative stress, inflammatory, and apoptotic induced damage (Afsar et al., 2020; El-Sayed et al., 2017; Songbo et al., 2019). As reported previously, both resveratrol and pirfenidone suppressed these damaging effects. Resveratrol plays an antioxidative role by scavenging DOX-induced oxygen radicals and inhibiting apoptosis (Rawat et al., 2021).

In the present study, resveratrol and pirfenidone exerted significant lowering of the inflammatory and apoptotic biomarkers: COX2, NO, TNF-α, and caspase-3, with amelioration of the histological damage induced by doxorubicin. It has also been reported that inflammation contributes to DOX-encouraged renal injury. In this study, DOX significantly raised the levels of proinflammatory mediators and cytokines, such as COX2, NO, and TNF-α. The role of inflammasomes in the inflammatory response has been demonstrated in numerous studies (Gu et al., 2021). In agreement with our findings, DOX enhances activation of NLRP3 inflammasomes with hypersecretion of IL-1β and caspase-1 and causes inflammatory effects, apoptosis, and oxidative stress in cardiomyocytes (Wang et al., 2016). Doxorubicin triggers the translocation of NF-κB to the nucleus by inducing the degradation of its inhibitory protein IkB-α. This activation of the NF-κB signaling pathway is subsequently accompanied by an elevated production of inflammatory mediators, including TNF-α (Kabel et al., 2021).

The inflammation process is closely associated with fibrosis. Many inflammatory mediators are released and contribute to the induction of fibrosis (profibrotic effects) or suppressing it (antifibrotic effects) (Xua et al., 2020). The final and typical pathological endpoint of many chronic inflammatory diseases is fibrosis. TGF-β1 is the master regulator molecule of fibrosis. TGF-β1 is a multifunctional cytokine that manages collagen formation and the deposition of collagen proteins in renal fibroblasts. Moreover, TGF-β1 is the principal controller of extracellular matrix protein deposition (Bolourani et al., 2021). Consistent with these facts, our results showed that doxorubicin leads to significant elevation of TGF-β1 gene expression with concomitant elevation of MMP-9 and reduction of PAS-stained renal tissue. Moreover, our results showed that resveratrol and pirfenidone exhibited a significant lowering effect on TGF-β, immunostaining of MMP-9, and increase of PAS-stained area. Our findings agree with a previous study which stated that resveratrol suppressed TGF-β expression and collagen deposition (Cheng et al., 2016).

It has been suggested that fibrosis plays a role in renal dysfunction associated with doxorubicin-induced renal toxicity. Fibroblasts exhibit an excessive production of collagen, which subsequently replaces the necrotic or apoptotic renal cells (Hazem et al., 2022a). In this current study, it was noted that doxorubicin-induced fibrosis promotes increased collagen deposition and elevated expression of MMP-9. MMP-9 not only serves as a key mediator in fibrosis but also functions as a promoter for organ fibrosis by facilitating extracellular differentiation and inducing epithelial–mesenchymal transition (Ashrafizadeh et al., 2020).

Our findings revealed a significant reduction in SIRT1 gene expression upon DOX administration. SIRT1, a NAD+-dependent deacetylase protein, influences the expression of various target proteins in tissues like the kidney, liver, muscle, and adipose tissue. SIRT1 is crucial in mitigating oxidative stress and exhibits protective effects against various diseases, including neurological, cancer, and renal conditions (Lohanathan et al., 2022). Multiple studies have demonstrated that activating SIRT1 is regarded as a cardioprotective approach in cardiovascular diseases, including DOX-induced cardiotoxicity (Rahman and Islam, 2011). In the present work, treatment with resveratrol and, pirfenidone increased SIRT1 gene expression. Previous studies showed that in rat animal models, resveratrol safeguards cardiac cells from myocarditis by increasing the expression of SIRT1, thereby diminishing apoptosis mediated through the FoxO1 pathway (Kuno et al., 2023).

Results of the present study showed that doxorubicin leads to upregulation of LncRNA (MALAT-1) gene expression. Metastasis-associated lung adenocarcinoma transcript 1 (MALAT1) is a long non-coding RNA (lncRNA) known to be deregulated, with prognostic and therapeutic implications identified in various cancers (Chen et al., 2009). Administration of either resveratrol or pirfenidone led to significant down-regulation of MALAT-1 gene expression. These findings coincided with previous studies that reported the effects of resveratrol or pirfenidone in suppressing the invasion and movement of cancer cells through inhibition of MALAT-1 mediated epithelial-to-mesenchymal transition (Syllaios et al., 2021; Yang et al., 2019). Study limitations include the small number of used animals and, the short-term effects of resveratrol and pirfenidone. It is recommended to conduct a future study for the long-term effects of these two drugs on chronic kidney damage such as diabetic nephropathy, hypertensive nephropathy, or long-term administration of doxorubicin.

5. Conclusions

In conclusion, doxorubicin induces deleterious effects on the renal tissue via upregulation of inflammatory mediators, oxidative stress markers, and apoptotic and fibrosis-related genes. The use of either pirfenidone or resveratrol showed significant anti-fibrotic and anti-oxidative effects in doxorubicin-exposed animals. Both therapeutic interventions elicited regulation and control of gene expression of Sirt-1, LncRNA (MALAT-1) gene, and TGFβ genes. It is recommended to conduct clinical trials on the combined therapy of pirfenidone and resveratrol with doxorubicin in different types of malignant tumors.

Conflict of interest

The authors state that they do not have any conflicts of interest.

Funding information

The authors affirm that they did not receive any financial support for conducting this study.

Data Availability

Data will be made available on request.

Acknowledgement

The authors would like to thank pathology department members.

References

Afsar, T., Razak, S., Almajwal, A., Al-Disi, D., 2020. Doxorubicin-induced alterations in kidney functioning, oxidative stress, DNA damage, and renal tissue morphology; improvement by *Acacia hydaspica* tannin-rich ethyl acetate fraction. Saudi J. Biol. Sci. 27 (9), 2251–2260. https://doi.org/10.1016/j.sjbs.2020.07.011.

Armendariz-Borunda, J., Lyra-González, I., Medina-Preciado, D., et al., 2012. A controlled clinical trial with pirfenidone in the treatment of pathological skin scarring caused by burns in pediatric patients. Ann. Plast. Surg. 68 (1), 22–28. https://doi.org/10.1097/SAP.0b013e31821b6d08.

Ashrafizadeh, M., Najafi, M., Orouei, S., et al., 2020. Resveratrol modulates transforming growth factor-beta (TGF-β) signaling pathway for disease therapy: a new insight into its pharmacological activities. Biomedicines 8 (8), 261. https://doi.org/10.3390/biomedicines8080261.

Beshay, O.N., Ewees, M.G., Abdel-Bakky, M.S., et al., 2020. Resveratrol reduces gentamicin-induced EMT in the kidney via inhibition of reactive oxygen species and involving TGF-β/Smad pathway. Life Sci. 258, 118178.

Bolourani, S., Brenner, M., Wang, P., 2021. The interplay of DAMPs, TLR4, and proinflammatory cytokines in pulmonary fibrosis. J. Mol. Med. 99, 1373–1384. https://doi.org/10.1007/s00109-021-02113-y.

Caraguel, C.G.B., Stryhn, H., Gagné, N., et al., 2011. Selection of a cutoff value for real-time polymerase chain reaction results to fit a diagnostic purpose: analytical and epidemiologic approaches. J. Vet. Diagn. Investig. 23 (1), 2–15. https://doi.org/10.1177/104063871102300102.

Cheng, W., Yan, K., Xie, L.Y., et al., 2016. MiR-143-3p controls TGF-beta1 induced cell proliferation and extracellular matrix production in airway smooth muscle via negative regulation of the nuclear factor of activated T cells 1. Mol. Immunol. 78, 133–139. https://doi.org/10.1016/j.molimm.2016.09.004.

Chen, Z.P., Mitchelhill, K.I., Michell, B.J., Stapleton, D., Rodriguez-Crespo, I., Witters, L. A., Power, D.A., de Montellano, P.R.Ortiz, Kemp, B.E., 1999. AMP-activated protein kinase phosphorylation of endothelial NO synthase. FEBS Lett. 443, 285–289 (View Article: Google Scholar: PubMed/NCBI).

Chen, J.F., Ni, H.F., Pan, M.M., et al., 2012. Pirfenidone inhibits macrophage infiltration in 5/6 nephrectomized rats. Am. J. Physiol. Ren. Physiol. 14 (6), 676–685. https://doi.org/10.1152/ajprenal.00507.2012.

Chen, C.J., Yu, W., Fu, Y.C., et al., 2009. Resveratrol protects cardiomyocytes from hypoxia-induced apoptosis through the SIRT1–FoxO1 pathway. Biochem. Biophys. Res. Commun. 378 (3), 389–393. https://doi.org/10.1016/j.bbrc.2008.11.110.

Cotino-Nájera, S., Herrera, L.A., Domínguez-Gómez, G., Díaz-Cháve, J., 2023. Molecular mechanisms of resveratrol as chemo and radiosensitizer in cancer. Front. Pharmacol. 14 https://doi.org/10.3389/fphar.2023.1287505.

Dolinsky, V.W., Chakrabarti, S., Pereira, T.J., Oka, T., Levasseur, J., Beker, D., Zordoky, B.N., Morton, J.S., Nagendran, J., Lopaschuk, G.D., et al., 2013. Resveratrol prevents hypertension and cardiac hypertrophy in hypertensive rats and mice. Biochim. Biophys. Acta 1832, 1723–1733 (View Article: Google Scholar: PubMed/NCBI).

Dolinsky, V.W., Morton, J.S., Oka, T., Robillard-Frayne, I., Bagdan, M., Lopaschuk, G.D., Des Rosiers, C., Walsh, K., Davidge, S.T., Dyck, J.R., 2010. Calorie restriction prevents hypertension and cardiac hypertrophy in the spontaneously hypertensive rat. Hypertension 56, 412–421 (View Article: Google Scholar: PubMed/NCBI).

Dou, Y., Zhao, D., 2022. Targeting emerging pathogenic mechanisms by natural molecules as potential therapeutics for neurodegenerative diseases. Pharmaceutics 14 (11), 2287.

El-Sayed, E.-S.M., Mansour, A.M., El-Sawy, W.S., 2017. Alpha lipoic acid prevents doxorubicin-induced nephrotoxicity by mitigation of oxidative stress, inflammation, and apoptosis in rats. J. Biochem. Mol. Toxicol. 31 (9), e21940 https://doi.org/10.1002/jbt.21940.

Faul, F., Erdfelder, E., Buchner, A., Lang, A.-G., 2009. Statistical power analyses using G* power 3.1: tests for correlation and regression analyses. Behav. Res. Methods 41, 1149–1160.

Fouad, H., Faruk, E.M., Alasmari, W.A., et al., 2021. Structural and chemical role of mesenchymal stem cells and resveratrol in the regulation of apoptotic-induced genes in Bisphenol-a induced uterine damage in adult female albino rats. Tissue Cell 70, 101502. https://doi.org/10.1016/j.tice.2021.101502.

Gu, T., Wang, N., Wu, T., et al., 2021. Antioxidative stress mechanisms behind resveratrol: a multidimensional analysis. J. Food Qual., 5571733 https://doi.org/10.1155/2021/5571733.

Den Hartogh, D.J., Tsiani, E., 2019. Health benefits of resveratrol in kidney disease: evidence from in vitro and in vivo studies. Nutrients 11, 1624. https://doi.org/10.3390/nu11071624.

Hazem, R.M., Antar, S.A., Nafea, Y.K., et al., 2022a. Pirfenidone and vitamin D mitigate renal fibrosis induced by doxorubicin in mice with Ehrlich solid tumor. Life Sci. 288, 120185 https://doi.org/10.1016/j.lfs.2021.120185.

Hazem, R.M., Antar, S.A., Nafea, Y.K., Al-Karmalawy, A.A., Saleh, M.A., El-Azab, M.F., 2022b. Pirfenidone and vitamin D mitigate renal fibrosis induced by doxorubicin in mice with Ehrlich solid tumor. Life Sci. 288, 120185.

Hekmat, S.A., Chenari, A., Alipanah, H., et al., 2021. Protective effect of alamandine on doxorubicin-induced nephrotoxicity in rats. BMC Pharm. Toxicol. 22, 31. https://doi.org/10.1186/s40360-021-00494-x.

Ikewuchi, C.C., Ifeanacho, M.O., Ikewuchi, J.C., 2021. Moderation of doxorubicin-induced nephrotoxicity in Wistar rats by aqueous leaf-extracts of *Chromolaena odorata* and *Tridax procumbens*. Porto Biomed. J. 6 (1), e129 https://doi.org/10.1097/j.pbj.0000000000000129.

ima-Posada, I., Fontana, F., Pérez-Villalva, R., et al., 2019. Pirfenidone prevents acute kidney injury in the rat. BMC Nephrol. 20, 158. https://doi.org/10.1186/s12882-019-1364-4).

Kabel, A.M., Salama, S.A., Adwas, A.A., Estfanous, R.S., 2021. Targeting oxidative stress, NLRP3 inflammasome, and autophagy by fraxetin to combat doxorubicin-induced cardiotoxicity. Pharmaceuticals *14*, 1188. https://doi.org/10.3390/ph14111188.

Kiernan, J.A., 2015. Immunohistochemistry. In: Kiernan, J. (Ed.), Histological and Histochemical Methods Theory and Practice, 4th ed. Scion Publishing Ltd,, pp. 454–490.

Kuno, A., Hosoda, R., Tsukamoto, M., et al., 2023. SIRT1 in the cardiomyocyte counteracts doxorubicin-induced cardiotoxicity via regulating histone H2AX. Cardiovasc. Res. 118 (17), 3360–3373. https://doi.org/10.1093/cvr/cvac026.

Liu, X., Su, C., Xu, J., et al., 2019. Immunohistochemical analysis of matrix metalloproteinase-9 predicts papillary thyroid carcinoma prognosis. Oncol. Lett. 17 (2), 2308–2316. https://doi.org/10.3892/ol.2018.9850.

Lohanathan, B.P., Rathinasamy, B., Huang, C.Y., Viswanadha, V.P., 2022. Neferine attenuates doxorubicin-induced fibrosis and hypertrophy in H9c2 cells. J. Biochem. Mol. Toxicol. 36 (7), e23054 https://doi.org/10.1002/jbt.23054.

Lopez, D.A., Sanchez, R.C., Montoya, B.M., et al., 2015. Role and new insights of pirfenidone in fibrotic diseases. Int. J. Med. Sci. 12 (11), 840–847. https://doi.org/10.7150/ijms.11579.

Mavrogiannis, E., Hagdorn, Q.A., Bazioti, V., Douwes, J.M., Van Der Feen, D.E., Oberdorf-Maass, S.U., Westerterp, M., Berger, R.M., 2022. Pirfenidone ameliorates pulmonary arterial pressure and neointimal remodeling in experimental pulmonary arterial hypertension by suppressing NLRP3 inflammasome activation. Pulm. Circ. 12 (3), e12101.

Miguel Andressa, F.P., Embaló, B., Alves Dias, H.B., Rivero, Elena R.C., 2021. Immunohistochemical expression of MMP-9, TIMP-1, and vimentin and its correlation with inflammatory reaction and clinical parameters in oral epithelial dysplasia. Appl. Immunohistochem. Mol. Morphol. 29 (5), 382–389. https://doi.org/10.1097/PAI.0000000000000910.

Morsi, A.A., Faruk, E.M., Mogahed, M.M., Baioumy, B., Hussein, A.Y., El-Shafey, R.S., Mersal, E.A., Abdelmoneim, A.M., Alanazi, M.M., Elshazly, A.M.E., 2023. Modeling the effects of cypermethrin toxicity on ovalbumin-induced allergic pneumonitis rats: macrophage phenotype differentiation and p38/STAT6 signaling are candidate targets of pirfenidone treatment. Cells 12 (7), 994.

Mozafari, M., Nekooeian, A.A., Panjeshahin, M.R., Zare, H.R., 2015. The effects of resveratrol in rats with simultaneous type 2 diabetes and renal hypertension: a study of antihypertensive mechanisms. Iran. J. Med. Sci. 40 (2), 152–160. PMID: 25821295; PMCID: PMC4359935).

Nade, V.S., Kawale, L.A., Bhangale, S.P., Wale, Y.B., 2013. Cardioprotective and antihypertensive potential of Morus alba L. in isoproterenolinduced myocardial infarction and renal artery ligation-induced hypertension. J. Nat. Remedies 13 (1), 54–67.

Pinkaew, D., Martinez-Hackert, E., Jia, W., et al., 2022. Fortilin interacts with TGF-β1 and prevents TGF-β receptor activation. Commun. Biol. 5, 157. https://doi.org/10.1038/s42003-022-03112-6.

Rahman, S., Islam, R., 2011. Mammalian Sirt1: insights on its biological functions. Cell Commun. Signal 9, 11. https://doi.org/10.1186/1478-811X-9-11.

RamachandraRao, S.P., Zhu, Y., Ravasi, T., et al., 2009. Pirfenidone is renoprotective in diabetic kidney disease. J. Am. Soc. Nephrol. 20 (8), 1765–1775. https://doi.org/10.1681/ASN.2008090931.

Rawat, P.S., Jaiswal, A., Khurana, A., et al., 2021. Doxorubicin-induced cardiotoxicity: an update on the molecular mechanism and novel therapeutic strategies for effective management. Biomed. Pharmacother. 139, 111708 https://doi.org/10.1016/j.biopha.2021.111708.

Shahbazi, F., Farvadi, F., Shojaei, L., et al., 2020. Potential nephroprotective effects of resveratrol in drug induced nephrotoxicity: a narrative review of safety and efficacy data. Adv. Tradit. Med. 1–16. https://doi.org/10.1007/s13596-020-00432-y.

Shao, Y., Luo, W., Guo, Q., et al., 2019. In vitro and in vivo effect of hyaluronic acid modified, doxorubicin and gallic acid co-delivered lipid-polymeric hybrid nano-system for leukemia therapy. Drug Des. Dev. Ther. 13, 2043–2055. https://doi.org/10.2147/DDDT.S202818.

Singh, A.P., Singh, R., Verma, S.S., et al., 2019. Health benefits of resveratrol: evidence from clinical studies. Med. Res. Rev. 39, 1851–1891. https://doi.org/10.1002/med.21565.

Songbo, M., Lang, H., Xinyong, C., et al., 2019. Oxidative stress injury in doxorubicin-induced cardiotoxicity. Toxicol. Lett. 307, 41–48. https://doi.org/10.1016/j.toxlet.2019.02.013.

Song, J.Y., Shen, T.C., Hou, Y.C., et al., 2020. Influence of resveratrol on the cardiovascular health effects of chronic kidney disease. Int. J. Mol. Sci. 21 (17), 6294.

Stojanović, D., Milenković, J., Veličkov, A., Ignjatović, A., Milojković, M., Dunjić, O., 2022. The emerging benefits of renalase based on preclinical studies: the current perspective. Acta Med. Median. 61 (4), 87–96.

Syllaios, A., Moris, D., Karachaliou, G.S., et al., 2021. Pathways and role of MALAT1 in esophageal and gastric cancer (Review). Oncol. Lett. 21, 343. https://doi.org/10.3892/ol.2021.12604.

Theodotou, M., Fokianos, K., Mouzouridou, A., Konstantinou, C., Aristotelous, A., Prodromou, D., Chrysikou, A., 2017. The effect of resveratrol on hypertension: a clinical trial. Exp. Ther. Med. 13 (1), 295–301.

Wang, L., Chen, Q., Qi, H., et al., 2016. Doxorubicin-induced systemic inflammation is driven by upregulation of toll-like receptor TLR4 and endotoxin leakage. Cancer Res. 76 (22), 6631–6642. https://doi.org/10.1158/0008-5472.CAN-15-3034.

Wennmalm, A., Benthin, G., Edlund, A., 1993. Metabolism and excretion of nitric oxide in humans. An experimental and clinical study. Circ. Res. 73, 1121–1127.

Wu, L.H., Qu, B., Wu, L., Liu, Y., et al., 2022. Can Resveratrol protect against renal ischemia/reperfusion injury? A systematic review and meta-analysis of preclinical studies. KIReports 7 (2), S23–S24. https://doi.org/10.1016/j.ekir.2022.01.063.

Xua, A., Dengb, F., Chenc, Y., Kongd, Y., et al., 2020. NF-κB pathway activation during endothelial-to-mesenchymal transition in a rat model of doxorubicin-induced cardiotoxicity. Biomed. Pharmacother. 130, 110525.

Yalcın, T., Kaya, S., Kuloğlu, T., 2023. Resveratrol may dose-dependently modulate nephrin and OTULIN levels in a doxorubicin-induced nephrotoxicity model. Toxicol. Mech. Methods 9, 1–11. https://doi.org/10.1080/15376516.2023.2268717.

Yalcın, Tuba, Kaya, Sercan, Kuloğlu, Tuncay, 2024. Resveratrol may dose-dependently modulate nephrin and OTULIN levels in a doxorubicin-induced nephrotoxicity model. Toxicol. Mech. Methods 34 (1), 98–108 doi: 10.1080/15376516.2023.2268717https://doi.org/10.1080/15376516.2023.2268717.

Yamazaki, T., Yamashita, N., Izumi, Y., Nakamura, Y., Shiota, M., Hanatani, A., Shimada, K., Muro, T., Iwao, H., Yoshiyama, M., 2012. The antifibrotic agent pirfenidone inhibits angiotensin II-induced cardiac hypertrophy in mice. Hypertens. Res. 35 (1), 34–40. https://doi.org/10.1038/hr.2011.139. Epub 2011 Aug 25. PMID: 21866107).

Yang, Z., Xie, Q., Chen, Z., et al., 2019. Resveratrol suppresses the invasion and migration of human gastric cancer cells via inhibition of ALAT1-mediated epithelial-to-mesenchymal transition. Exp. Ther. Med. 17, 1569–1578. https://doi.org/10.3892/etm.2018.7142.

Zhang, J., Xie, Z., Dong, Y., Wang, S., Liu, C., Zou, M.H., 2008. Identification of nitric oxide as an endogenous activator of the AMP-activated protein kinase in vascular endothelial cells. J. Biol. Chem. 283, 27452–27461 (View Article: Google Scholar: PubMed/NCBI).